Magnetic properties of Gd-Y alloys: Regularities and anomalies

M. Foldeaki, R. Chahine, and T. K. Bose
Institut de Recherche sur l'Hydrogène, Université du Québec à Trois-Rivières, Québec, Canada G9A 5H7
(Received 31 October 1994; revised manuscript received 8 March 1995)

The Gd-Y system was investigated in the 0–67 at. % Y concentration range between 4.2 and 350 K, in external fields up to 1 T. The effective paramagnetic moment on Gd atoms was found to be concentration dependent, with a maximum of $9.13\mu_B$ at 40.1 at. % Y. Ordered moments on Gd atoms at 5 K showed similar behavior. The observed behavior is consistent with the assumption that Y changed the anisotropy of the crystal field acting on the Gd atoms, resulting in increased total angular momentum. Magnetization data were analyzed to give the thermodynamic transition temperature and the zero-field specific-heat anomaly at the transition. Simultaneously, the change in magnetic entropy for 1 T field was calculated. The magnetic entropy change was found to be nearly concentration independent in the concentration range of increasing Gd atomic magnetic moment. For higher Y contents, the magnetic entropy change sharply decreases. The calculated specific-heat anomaly likewise decreases above 10 at. % Y, and cannot be evaluated for alloys with prevailing helimagnetic structure. The results are in good qualitative agreement with the magnetic phase diagram, obtained via neutron diffraction, although present magnetic measurements provide more details on the critical fields.

I. INTRODUCTION

Rare-earth metals, alloys, and compounds have been studied extensively for their complex magnetic structures, as summarized in several monographs.[1–5] However, the thermal properties in the vicinity of the magnetic transition temperature, such as the isothermal entropy change upon magnetization and the discontinuity of the specific heat, have not been investigated in detail yet. As was shown in an earlier paper,[6] magnetic measurements performed up to 1 T applied field allow us to calculate the isothermal entropy change and the specific-heat anomaly at the transition. Simultaneously, the results allow us to characterize the symmetry of the magnetic order below the transition.

We had chosen to study the Gd-Y system, because a solid solution alloy with a nonmagnetic diluent might facilitate the understanding of the composition dependence of the magnetic properties. In earlier studies,[7–12] several magnetic structures and transitions had been found. The dilution with yttrium tends to stabilize the antiferromagnetic spiral structure at the expense of the ferromagnetic order present in gadolinium. Some of the studies[7,8] observed an excess moment on Gd atoms, both in paramagnetic and ferromagnetic phases, which has been attributed either to a polarization of the conduction band or to a change of spin-orbit interaction, although no systematic investigation has been carried out and the observation has not been correlated to the composition or other magnetic properties. The magnetic phase diagram exists between 20 and 40 at. % Y. Below 30 at. %, the high-temperature ordered phase corresponds to a *c*-axis ferromagnet, with disorder in the basal plane, which transforms into a simple canted structure, where the cant angle increases with increasing Y content.[10,12] This results in an orientation-dependent Curie temperature, and might appear as a double Curie point in polycrystals.

Above 30 at. % Y the *c*-axis ferromagnet is replaced by a simple helical phase (where the moments are confined to the hexagonal basal plane), while the lower-temperature canted ferromagnetic phase is still present up to 40 at. % Y. The results suggest[10,11] that no ferromagnetic phase is present above 40 at. %. Near 30 at. % Y, small applied fields are sufficient to suppress the helical structure.[12]

Goals of the present study include investigation of magnetic properties in a broader composition range than previously reported, and to correlate different magnetic properties with each other and the composition.

II. EXPERIMENTAL METHODS

A. Sample processing

The alloys of gadolinium and yttrium were prepared in an arc furnace. Both Gd and Y were of 99.8% purity. The concentration of metallic impurities was less than 0.01% each, with the exception of Ta, which was about 0.1%. The starting materials contained about 0.04–0.06 wt % oxygen. The required amounts of Gd and Y were placed into the water-cooled copper hearth, that doubled as the positive electrode. The alloy was melted in an argon atmosphere using a thin tungsten rod as a negative electrode. After the first melting, the ingot was flipped over and remelted repeatedly to ensure homogeneity in the alloy. The loss was minimal in all cases and gas analysis did not reveal a change of oxygen concentration. Thus, a good agreement between the nominal and the actual compositions can be expected. Samples for super-

conducting quantum interference device (SQUID) magnetometry were cut using a precision diamond saw.

B. Materials testing

The homogeneity and correct composition of the samples were tested using conventional metallography followed by scanning electron microscopy with an energy-dispersive composition analyzer. No second phases or significant inhomogeneities were found. The standardless composition analysis qualitatively confirmed the composition (increasing nominal compositions resulted in increased nominal signals) and revealed only $\pm 1.5\%$ deviations as a function of beam location. The low loss during melting, the homogeneity, and the qualitative agreement found by the standardless analysis justified the use of nominal compositions in further calculations.

C. Magnetic measurements

All the magnetic measurements were carried out in a 1 T Quantum Design SQUID magnetometer. First, susceptibility curves at 0.0025 and 1 T were measured over the total temperature range. Their comparison indicated the nature of the magnetic order present. The low-field susceptibility curve was used to identify the transition region in which a set of about 20 magnetization curves was measured. The temperature steps were 2.5 K apart closer to the transition and 5 K further away. These magnetization curves were used to calculate the thermodynamic parameters and the magnetic entropy change. Curie-Weiss parameters were calculated from the 1 T susceptibility curve.

III. EXPERIMENTAL RESULTS

A. Magnetic susceptibility and hysteresis

No significant hysteresis has been found in any of the samples in the investigated temperature ranges. Figure 1 displays susceptibility versus temperature curves, as measured in low (0.0025 T) and high (1 T) field. As a function of the yttrium content, the following qualitative tendencies can be observed: The behavior shown in Fig. 1(a) is characteristic for low Y contents (below 30 at. %). The high-temperature transition, manifested as a sharp peak on the low-field curve, shifts toward lower temperature with increasing yttrium content, indicating a decrease of the exchange interactions. The difference between low- and high-field susceptibilities is about one order of magnitude, the high-field susceptibility being lower. The high-field curve does not show a peak at the transition temperature. This behavior is typical for simple ferromagnets.

With increasing Y contents, two transitions are present and the field dependence becomes more complex. In the low-field curve [Fig. 1(b)], there appear two peaks. The lower-temperature peaks indicate a ferromagnetic/antiferromagnetic phase transition, while the higher-temperature peak is connected to an antiferromagnetic/paramagnetic transition. The high-field curve displays only the higher-temperature transition in the form of a sharp decrease of the susceptibility, indicating that higher fields completely suppressed the antiferromagnetic phase. When the Y level further increases [Fig. 1(c)], the higher-temperature peak connected to the antiferromagnetic/paramagnetic transition increases and is manifested in the high-field curve as well, indicating that the antiferromagnetic phase can no more be suppressed by high fields. The difference between the low- and high-field curves decreases, indicating the changing nature of response to magnetic fields. This behavior is usual in noncollinear magnetic structures, uniquely present above 40 at. % Y. In this helimagnetic regime, we observe a rather well-defined susceptibility maximum at low temperatures, which might indicate the transition to the low-temperature ferromagnetic phase. In this study, we investigated only the upper transition in detail.

In the ferromagnetic regime, we do not see a clear indi-

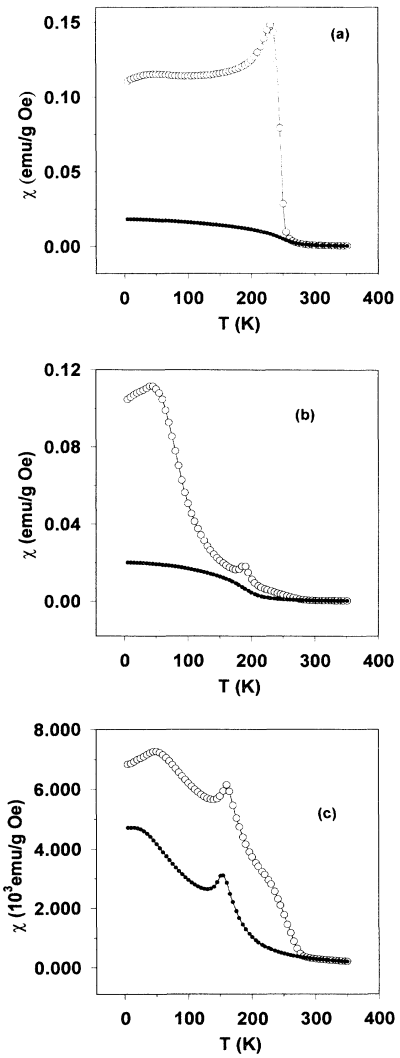

FIG. 1. Low (0.0025 T, ○) and high (1 T, ●) field susceptibilities characteristic for (a) low (0–30 at. %), (b) medium (30–45 at. %), or (c) high (>45 at. %) yttrium contents. Solid lines are guiding the eye.

cation for the presence of "double" ferromagnetism.[12] As we are measuring on polycrystals, where differences in magnetic behavior of different orientations are averaged out, this is no surprise. Also, our measuring field is higher than that applied in the earlier study.[12] Only one phenomenon indicates the presence of an anomaly: The temperature of the susceptibility peak is significantly lower than calculated from the Curie-Weiss or thermodynamic parameters.

The Curie (C) and Weiss (Θ) constants were calculated from the high-field susceptibility in the usual way[13] and Table I shows the Weiss constants Θ and the effective atomic moments calculated from the Curie constant C. p_{eff}(avr) was calculated under the assumption that all atoms carry the same magnetic moment, while p_{eff}(Gd) corresponds to the magnetic moment of Gd atoms if $p_{\text{eff}}(Y)=0$. p_{eff}(calc) gives the average moment calculated from the nominal composition assuming p_{eff}(Gd) $=7.98\mu_B$ and $p_{\text{eff}}(\text{Y})=0$.

Weiss constants display a monotonous decrease with composition as observed in other studies as well.[1] The calculated average atomic moments, on the other hand, show a very different qualitative tendency. Figure 2 displays the average effective atomic moments as a function of the Y content. The dotted line gives the theoretical value. Comparing the experimental and theoretical curves, a systematic deviation appears. Although the experimental error is about $\pm 1.5\%$, including composition fluctuations, the tendency for a nonmonotonous dependence is present without doubt: The effective atomic moment shows a maximum around 40 at. % Y and the same tendency can be observed in the Gd atomic moments in Table I, last column.

B. Transition temperature and specific-heat anomaly

The theory for the second-order phase transition[14,15] predicts the following relation between the high-field magnetization ("approach to saturation") and the external field near the transition temperature:

$$\alpha+\beta M^2=H/M \ . \tag{1}$$

Consequently, the measured M versus H curves were transformed into H/M versus M^2. When H/M is plotted as a function of M^2, the relationship is linear in the region of the true magnetization. The experimental points in this section were fitted to a linear least-squares program. The resulting α and β parameters were used to calculate the thermodynamic Curie point and the specific-heat anomaly at the Curie point. The Curie point is obtained by a linear fit to the $\alpha=\alpha'_{\Theta}(T-\Theta)$ equation. The specific-heat anomaly equals $\Delta C_p=(\alpha'_{\Theta})^2\Theta/2\beta(\Theta)$. Details were given elsewhere.[6] The error in the Curie point is about $\pm 1\%$, while the error estimate for the specific-heat anomaly is about $\pm 6\%$. We have to mention that this calculation and error estimate are strictly valid only for single-phase magnetic materials. For multiphase materials, especially if several ordered magnetic phases with different transition temperatures are present, the error has to be estimated individually.

A similar equation, obtained on the basis of the molecular field theory, was used by Arrott[16] to determine the onset of ferromagnetism (Curie temperature). The transition temperatures and specific-heat anomalies, as obtained from the above thermodynamic method, are also summarized in Table I.

Analysis according to Eq. (1) can be easily carried out

TABLE I. Composition, magnetic, and thermomagnetic parameters of the alloys investigated. n/a indicates that the value was not available (field too low).

Y (at. %)	de Gennes factor G	Weiss constant calculated from G Θ_{calc} (K)	Atomic moment calculated from Y content p_{eff}(calc) (μ_B)	Experimental Weiss constant Θ_{pm} (K)	Experimental average atomic moment from the Curie constant p_{eff}(avr) (μ_B) ($\pm=1.5\%$)	Experimental transition temperature from Arrott plots Θ_{fm} (K) ($\pm 1\%$)	Maximal magnetic entropy change $\Delta S_M^{(\max)}$ (J/kg K) ($\pm 7.5\%$)	Temperature at $\Delta S_M^{\max}$ T_{fm} (K)	Specific-heat anomaly at the transition ΔC_p (J/kg K) ($\pm 6\%$)	Experimental atomic moment on Gd only, from the Curie constant p_{eff}(Gd) (μ_B) ($\pm 1.5\%$)
0.0	15.75	289	7.89[a]	295.1	8.05	290.5	3.25	291.0	124	8.05
9.62	14.23	270.2	7.59	268.9	7.58	271.0	2.93	267.5	110	7.88
19.7	12.64	249.7	7.15	255.7	7.02	245.5	2.05	242.5	52	7.83
25.2	11.78	234.3	6.90	248.8	7.19	235.2	2.03	232.5	37	8.31
29.0	11.21	226.7	6.72	237.9	7.04	224.7	2.00	222.5	44	8.33
31.7	10.72	220.1	6.59	231.7	7.08	217.1	2.50	216.3	55	8.55
36.7	10.00	210.3	6.35	216.5	6.93	198.7	2.11	198.8	46	8.69
40.1	9.43	202.3	6.18	207.2	7.07	185.6	1.67	193.3	33	9.13
44.9	8.68	191.5	5.92	187.6	6.54	172.3	0.89	178.8	n/a	8.81
47.3	8.30	185.9	5.79	194.9	6.39	166.7	0.98	181.3	n/a	8.78
49.5	7.95	180.7	5.67	180.9	6.43	161.3	0.59	173.8	n/a	9.05
52.4	7.50	173.9	5.51	175.0	5.91	146.3	0.37	168.8	n/a	8.55
57.2	6.74	164.1	5.22	146.3	5.51	143.0	0.19	158.8	n/a	8.43
66.9	5.21	138.3	4.59	119.5	4.82	90.7	0.08	137.5	n/a	8.39

[a]Reference 2.

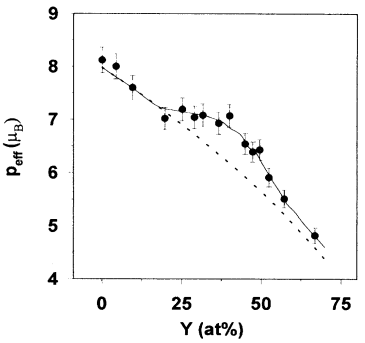

FIG. 2. Average effective atomic moments as a function of the composition. Solid lines are guiding the eye; dotted lines display theoretical values.

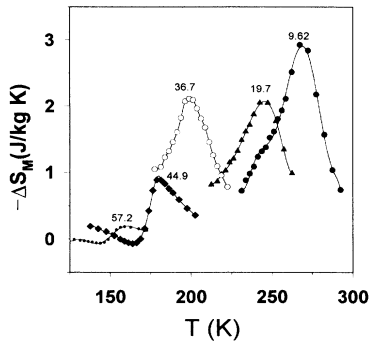

FIG. 3. Magnetic entropy change for $H=1$ T applied field, as a function of the temperature, for 9.62 (●), 19.7 (▲), 36.7 (○), 44.9 (■), and 57.2 (small ●) at. % Y, as denoted by numbers near the peaks. Solid lines are guides to the eye.

for low Y concentrations (up to about 30 at. %). In this range, the transformed H/M versus M^2 curves all have linear sections with $\beta>0$. For higher Y concentrations, the linear section of the low-temperature H/M versus M^2 curves might be characterized with a negative β, in contradiction to the thermodynamic theory. Changes in the magnetic order result in changes of the linear temperature dependence of the parameter α, making further evaluations difficult or impossible. In the ferromagnetic range (up to 30 at. % Y), deviations from linear can be observed only at low temperature, where the assumptions of the theory are not valid yet. In the vicinity of the transition, the α parameters form a single line, allowing an unambiguous determination of the transition temperature and the specific-heat anomaly. With increasing Y content, the α versus T function displays a more pronounced curvature. Up to about 45 at. % Y, the region near the transition can still be approximated linearly, although this results in an increased error in the specific-heat anomaly calculation. With further increase in the Y content, the linear section moves to higher temperatures. At the extrapolated transition temperature the theory is not yet valid ($\beta<0$), and consequently the specific-heat anomaly cannot be calculated. At the same time, the extrapolated transition temperature tends to be very different from the Weiss constant or the predicted transition temperature $T_N=46G^{2/3}$, where G is the de Gennes constant.[1,2] Sufficiently high fields, which saturate the sample after the helimagnetic-ferromagnetic transition, would allow thermodynamic calculations even in this composition range. Values of the specific-heat anomaly, where applicable, are summarized in Table I as a function of the Y content.

C. Magnetic entropy change

From the magnetization data, the magnetic entropy change for isothermal magnetization can be calculated as well. Due to the slow increase of the magnetic field in the superconducting magnet, the conditions can be considered as isotherm, rather than adiabatic. The entropy change associated with the change of the magnetization is given as[17]

$$\Delta S_M=\int_0^H\left[\frac{\partial M}{\partial T}\right]_H dH\ . \tag{2}$$

Theoretically, this value can be calculated from the molecular-field theory, which might not be valid for other than simple ferromagnetic order. The above equation, however, remains valid in general, as it is a thermodynamic result and no assumption was made on specific magnetic properties.

Figure 3 shows typical entropy curves for low and high Y contents, respectively. Up to about 40 at. % Y, the entropy curves remain qualitatively similar to that of Gd, although the maximum value displays slow, stepwise decrease with increasing Y content. At higher Y contents (>40 at. %), the maximum entropy change rapidly approaches zero and there appears a negative maximum on the low-temperature side of the entropy change vs temperature curves.

IV. DISCUSSION

A. Effective magnetic moments

Figure 2 displays the effective average atomic moments as calculated from the Curie constant. The ordered moment μ_s on the Gd atoms was estimated from the 5 K, 1 T magnetization using the relationship of $M/N=\mu_s$, where N equals the number of Gd atoms and M is the measured magnetization. The results are shown in Fig. 4(a). This approximation is valid for alloys which are ferromagnetic at low temperature. In the nonferromagnetic regime, either neutron diffraction or higher fields would be needed to reveal the ordered helimagnetic moment. Points corresponding to nonsaturated alloys are given by gray symbols in Fig. 4(a).

It is seen that the experimentally determined values of both the disordered (paramagnetic) and ordered (spontaneous) magnetic moments are significantly higher in certain composition ranges than the theoretical values for Gd obtained under the assumption of contributions by spin only. These are,[1] respectively, $p_{\text{eff}}=g[J(J+1)]^{1/2}=7.94$ and $\mu_s=gJ=7.00$ in bohr magnetons, where for

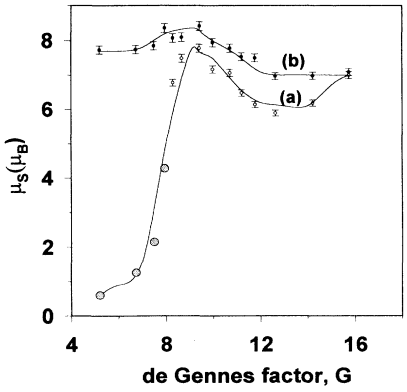

FIG. 4. Ordered magnetic moment of Gd atoms, as a function of composition calculated from (a) the 5 K saturation, or from (b) the effective λ and J. Gray points in (a) indicate values calculated from the 5 K, 1 T magnetization of nonsaturated samples. Solid lines are guiding the eye.

Gd $g=2$ and $J=\frac{7}{2}$. Although the same tendency has been observed by other authors as well,[7,8] it contradicts theoretical expectations: The $4f$ shell, which contains the electrons of unpaired spins in the rare earths, is so well shielded by outer electrons that the direct interaction between the $4f$ electrons of neighboring atoms must be small. Yttrium, the trivalent fourth-period element has the same crystal structure as Gd and nearly the same atomic volume. This close similarity would indicate that yttrium should be an ideal diluent[7] for Gd, i.e., substituting Y for Gd should only result in a reduction of the exchange field due to dilution, but should not change the crystal field or the conduction electron polarization. On the contrary, it appears that the presence of the Y either brings into play contributions to magnetism by orbital moments (i.e., changes the crystal field), or alters the probability of transfers from the conduction-band electrons in a manner favoring an increased magnetic moment.

From the de Gennes factor, and p_{eff} associated with Gd moments only, an effective Lande factor λ and effective J have been calculated. The results are plotted in Fig. 5. Using this λ and J to calculate the ordered moment at low temperatures, we get a good agreement with experimental results in the ferromagnetic region, justifying the empirical approach [curve (b) in Fig. 4]. The decrease of the effective λ and simultaneous increase of the effective J are compatible with the assumption that the presence of certain amounts of Y changed the crystal field, thus favoring spin/orbit interactions on the Gd atoms. As the increase is present in the paramagnetic range as well, conduction electron polarization is unlikely. The increase in the atomic moment is the most pronounced in the composition range where helimagnetism and ferromagnetism coexist at low temperatures. It seems that an instability of the magnetic structure is connected to the increased magnetic moment. No increase could be observed in the composition range with ferromagnetic order, and a slow decrease is observed above 40 at. % Y,

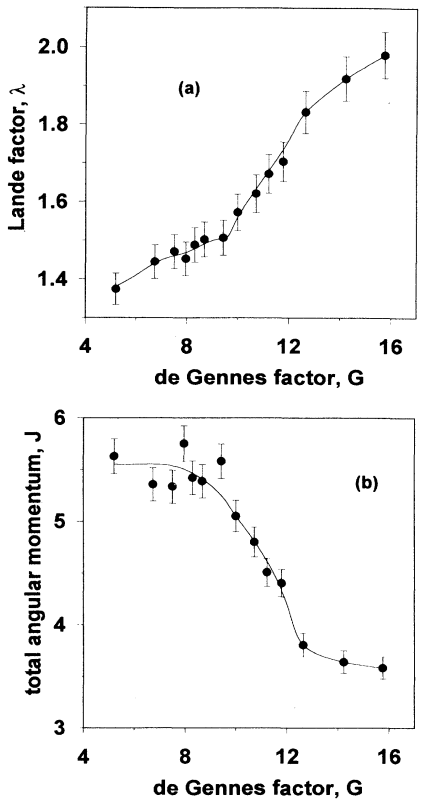

FIG. 5. (a) "Effective" Lande factor λ and (b) J as a function of composition, as calculated from G and p_{eff}.

where helimagnetism becomes the only ordered magnetic phase. A quantitative or even a more exact qualitative interpretation cannot be given at present.

B. Transition temperature

Unlike the magnetic moments, the transition temperatures at Gd-Y alloys display a monotonous concentration dependence. As shown in Table I, the Weiss constant, Θ_{pm}, the transition temperature obtained from the Arrott plots, Θ_{fm}, and the temperature of the maximum of magnetic entropy change, T_{fm}, show good agreement in the ferromagnetic range of composition, but display significant differences at higher Y contents. In further evaluation, we used the temperature of the maximum entropy change as the transition temperature. In an earlier study we found that this shows a good coincidence with the real transition temperature even for noncollinear structures.[6] In Fig. 6, this temperature is plotted as a function of composition. The small symbols correspond to the Gd-Y magnetic phase diagram, obtained via neutron diffraction,[10] while the larger symbols result from this study. The solid line is a guide to the eye, while the dotted line displays the $G^{2/3}$ dependence. Figure 6 displays a good agreement between our result and the magnetic phase diagram, both indicating a deviation from the $G^{2/3}$ empirical relationship, which is otherwise valid for most rare-earth/rare-earth alloys. Similar devi-

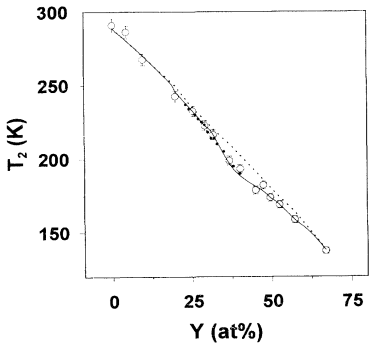

FIG. 6. Upper transition temperature as a function of composition. Dotted line corresponds to values calculated from the empirical equation $T_2=46G^{2/3}$ (Ref. 3). Large symbols correspond to the maximal magnetic entropy change; small symbols were obtained via neutron diffraction (Ref. 10).

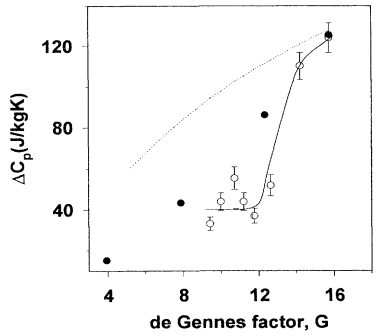

FIG. 7. Specific-heat anomaly as a function of the G factor. Open symbols were calculated from our magnetic data (Refs. 14, 15); full symbols correspond to calorimetric measurements (Ref. 18). Dotted line displays the behavior predicted by the molecular field. Solid lines are guides to the eye.

ations were already found,[1] leading to the conclusion that rare-earth Y alloys behave in many ways more anomalous than intra-rare-earth solid solutions.

Table I reveals that the composition dependence of the transition temperatures obtained as the maximum of the magnetic entropy change $T_{\rm fm}$ or from the method of the thermodynamic parameters, $\Theta_{\rm fm}$ agree within limits of error in experiment and evaluation up to 36.7 at. % Y. At higher Y concentrations (above 40.1%), the difference increases. As the value connected to the entropy change agrees with the phase diagram and calculated values, we have to conclude that the error in the method of the thermodynamic parameters increased in the helimagnetic phase. Most probably, the applied 1 T field does not saturate the helimagnetic alloys; consequently, the extrapolation is no longer valid. Studies in higher field are on the way.

C. Specific-heat anomaly

We stress that the specific-heat anomaly is calculated this way from *experimental* magnetization data, and no assumption is made regarding the magnetic order. The molecular-field theory, based on simple ferromagnetic order, predicts the specific-heat anomaly as a function of the number of magnetic moments present and the magnitude of the moment. The equation obtained for the value of the anomaly at the transition temperature is[17]

$$\Delta C_p = Nk\frac{5j(j+1)}{j^2+(j+1)^2}\ , \tag{3}$$

where N is the number of magnetic atoms, j their angular quantum number, and k the Boltzmann constant.

On this basis, the specific heat anomaly can be calculated from the effective J values, based on the number of Gd atoms in the alloy. As Fig. 7 shows, the specific-heat anomaly calculated from Eq. (3) displays a gradual, monotonous decrease. On the contrary, the value obtained from magnetization data indicates a sharp decrease, followed by an oscillatory behavior around a constant value. Below $G\sim 10$, the specific-heat anomaly cannot be calculated from magnetic data as the field was no longer sufficient to saturate the sample. The low plateau in the specific-heat anomaly appears in the same composition range where we observe a maximum in the effective atomic moments. Calorimetric measurements[18] reveal a composition dependence similar to that observed in this study (Fig. 7, full symbols), although the values are somewhat higher than ours, especially for intermediate Y concentrations. The discrepancy might be caused by the nature of the samples and measurement: Calorimetric measurements at zero field thus obtain the true helimagnetic/paramagnetic transition, while our data are extrapolated from the ferromagnetic range. However, both data display the same tendency and the qualitative agreement is good.

Single crystals display double specific-heat anomaly peaks in alloys with "double" ferromagnetism,[12] i.e., in a narrow composition range around 30 at. % Y. Although the effect should be present in polycrystals, it had not been found by calorimetry;[18] neither did we observe it. Its absence in the calorimetric measurements[18] might be due to the fact that the narrow composition range of double ferromagnetism near 30 at. % Y was not investigated. In our case, magnetic measurements on polycrystals are not expected to reveal orientation-dependent Curie points. Their presence, however, might introduce errors into the evaluation according to the thermodynamic parameters, as only the macroscopic magnetization can be measured, while evaluation should be done independently for the two directions. Unequal contributions from $M\|a$ or c might well distort the linear dependence (or change the slope), and thus be responsible for the observed ambiguity (increased experimental error) in the specific-heat anomaly.

D. Magnetic entropy change and critical field

Different compositions show characteristic differences in the field and temperature dependence of the magnetic entropy change. For low Y concentrations, the entropy change is a monotonously decreasing function of the field [Fig. 8(a)]. The slope is increasing with the temperature

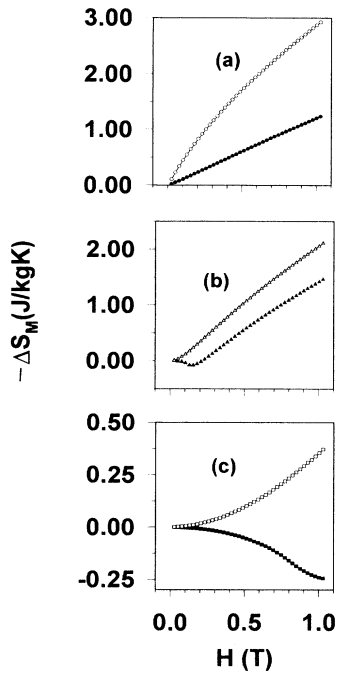

FIG. 8. Characteristic field dependence of the magnetic entropy change for (a) typically ferromagnetic alloys (shown 9.62 at. % Y at 241 K, ●, and at 267.5 K, ○), (b) alloys with transition (shown 36.7 at. % Y, at 189 K, ▲, and 200 K, △), and (c) typically helimagnetic alloys (shown 52.4 at. %, 154 K, ■, and 169 K, □). Solid lines are guides to the eye.

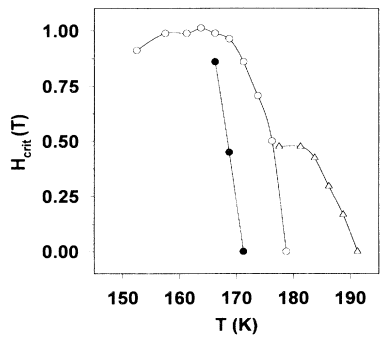

FIG. 9. Critical fields (crossover fields) versus temperature in the intermediate composition range: 49.5 at. % Y, (●), 44.9 at. % Y, (○), and 40.1 at. % Y, (△). For more details, see text.

below the transition, and decreases above, but the character of the function remains the same. Well below the transition, the field dependence of the magnetic entropy change is nearly linear. In the medium Y concentration range, and far below the transition temperature, the entropy change is positive first, and becomes negative only at higher fields [Fig. 8(b)]. With increasing temperature, the behavior becomes similar to that of ferromagnets. Alloys with high Y content do not show a linear behavior in any investigated field or temperature range. Far below the transition, the change is positive in the total field range and it becomes negative only in the immediate vicinity of the transition, where its field dependence is still slower than linear or what is observed for lower concentrations [Fig. 8(c)]. The observed behavior of the magnetic entropy change can be qualitatively well understood on the basis of the magnetization behavior of a helimagnet.[4] In weak fields, the entropy increases because upon magnetization the field destroys the existing symmetry of the helimagnetic system. With increasing field, one ultimately arrives at a ferromagnetic structure, whose symmetry and order parameter are superior to those of helimagnets. At a temperature-dependent critical field, a first-order transition from the helimagnetic fan structure to ferromagnetism takes place, resulting in a sharp decrease of the entropy, followed by further decrease with increasing field [Fig. 8(b)]. Near the transition temperature, the field dependence of the magnetic entropy change is linear in the investigated field range. The field of the crossover (where the magnetic entropy change changes sign) is defined as the critical field, although it might not be necessarily equal to that found from single-crystal or neutron-diffraction measurements. In Fig. 9 this field is plotted as a function of the temperature. For alloys above 49.5 at. % Y, it is above 1 T in the total temperature range below the transition and sharply falls to zero at the transition. For ferromagnetic alloys, it is zero in the total investigated range. For intermediate compositions, it forms a broad plateau below the transition, gradually decreasing as the temperature approaches the Curie point. The height of the plateau increases with increasing Y concentration. We did not observe the sharp maximum reported by Andreenko *et al.*,[19] although some samples indicate a tendency for decreasing critical fields at the lower-temperature end of the plateau, probably due to the proximity of a low-temperature ferromagnetic phase. This phenomenon was not investigated in detail. Detailed investigations over the total temperature range of the helimagnetic structure with higher applied fields (9 T) are on the way and will be reported soon.

E. Magnetic phase diagram

The investigated parameters indicate that the helimagnetic phase becomes stable at about 40 at. % Y, i.e., for $G \approx 10$. On the contrary, measurement and calculation of the turn angle[2,5] obtained a phase boundary at $G = 12$. The discrepancy is caused by an instability of the structures present to applied field. Calculations[5] and neutron diffraction[2] were both carried out in zero field. Our investigations indicate the presence of a helimagnetic phase with vanishing critical field for $10 < G < 12$ and another with high critical fields above $G = 12$, adding more fine details to the already known magnetic phase diagram.

ACKNOWLEDGMENTS

We would like to thank Mr. Arezki Smaili for his assistance with some of the experiments. This work was supported by Natural Resources of Canada and Ressources naturelles du Québec.

[1]R. J. Elliott, in *Magnetism,* edited by G. T. Rado and H. Suhl (Academic, New York, 1965), Vol. II, Pt. A, pp. 385–424.
[2]J. J. Rhyne, in *Magnetic Properties of Rare Earth Metals,* edited by R. J. Elliott (Plenum, London, 1972), Chap. 4, p. 129.
[3]W. C. Koehler, in *Magnetic Properties of Rare Earth Metals* (Ref. 2), Chap. 4, p. 81.
[4]R. Cooper, in *Magnetic Properties of Rare Earth Metals* (Ref. 2), Chap. 2, p. 17.
[5]K. N. R. Taylor and M. I. Darby, *Physics of Rare-Earth Solids* (Chapman and Hall, London, 1972).
[6]M. Foldeaki, R. Chahine, and T. K. Bose, J. Appl. Phys. **77**, 3528 (1995).
[7]W. C. Thoburn, S. Legvold, and F. H. Spedding, Phys. Rev. **110**, 1298 (1958).
[8]H. R. Child and J. W. Cable, J. Appl. Phys. **40**, 1003 (1969).
[9]R. J. Melville, S. B. Palmer, S. Bates, and G. J. McIntyre, J. Magn. Magn. Mater. **116**, 267 (1992).
[10]S. Bates, S. B. Palmer, J. B. Sousa, G. J. McIntyre, D. Fort, S. Legvold, B. J. Beaudry, and W. C. Koehler, Phys. Rev. Lett. **55**, 2968 (1985).
[11]S. B. Palmer, S. Bates, G. J. McIntyre, J B. Sousa, D. Fort, and B. J. Beaudry, J. Magn. Magn. Mater. **54-57**, 519 (1986).
[12]S. Legvold, T. Ito, and B. J. Beaudry, Phys. Rev. Lett. **45**, 1275 (1980).
[13]B. D. Cullity, *Introduction to Magnetic Materials* (Addison-Wesley, Reading, MA, 1972).
[14]L. D. Landau and E. M. Lifschitz, *Physique Statistique,* Traduction Française Pt. 1 (Editions Mir, Moscow, 1984).
[15]K. P. Belov, *Magnetic Transitions* (Boston Technical, Cambridge, 1965).
[16]A. Arrott, Phys. Rev. **108**, 1394 (1957).
[17]R. Becker and W. Doring, *Ferromagnetismus* (Springer-Verlag, Berlin, 1939).
[18]G. A. Costa and E. Kaiser, Thermochim. Acta **227**, 107 (1993).
[19]A. S. Andreenko, K. P. Belov, S. A. Nikitin, and A. M. Tishin, Sov. Phys. Usp. **32**, 649 (1989).